FERMILAB-CONF-15-538-PPD
ACCEPTED

EPJ Web of Conferences will be set by the publisher
DOI: will be set by the publisher
© Owned by the authors, published by EDP Sciences, 2015

Exclusive Central $\pi^+\pi^-$ Production in Proton Antiproton Collisions at the CDF

Maria Zurek[1,2,a]
on behalf of the CDF Collaboration

[1] *Forschungszentrum Jülich, 52425 Jülich, Germany*
[2] *University of Cologne, 50937 Cologne, Germany*

Abstract. Exclusive $\pi^+\pi^-$ production in proton-antiproton collisions at $\sqrt{s} = 0.9$ and 1.96 TeV in the Collider Detector at Fermilab has been measured. We select events with two particles with opposite charge in pseudorapidity region $-1.3 < \eta < 1.3$ with no other particles detected in $-5.9 < \eta < 5.9$. Particles are assumed to be pions. The $\pi^+\pi^-$system is required to have rapidity $-1.0 < y < 1.0$. The data are expected to be dominated by the double pomeron exchange mechanism. Therefore, the quantum numbers of the central state are constrained. The data extend up to dipion mass $M(\pi^+\pi^-) = 5000$ MeV/c^2. Resonance structures consistent with f_0 and $f_2(1270)$ mesons are visible. The results are valuable for light hadron spectroscopy and for providing information about the nature of the pomeron in a region between non-perturbative and perturbative quantum chromodynamics.

1 Introduction

Diffraction processes with low momentum-transfer squared, i.e., elastic scattering of protons at high energies, cannot be described by perturbative quantum chromodynamics, and the nonperturbative methods have to be involved. Elastic scattering and other diffractive interactions are described in the regime of Regge theory [1, 2] by the exchange of a pomeron, $\mathbb{P}$, which is a strongly interacting color-singlet. At leading order it is a pair of gluons [1]. Such processes are characterized by a region of large rapidity gaps, Δy, with no hadron production. With the requirements of two large rapidity gaps and central hadrons production, it is expected that the observed processes are dominated by double pomeron exchange, D$\mathbb{P}$E [1, 2].

In our work, central exclusive production is defined as a reaction $p\bar{p} \to p^{(*)}+GAP+X+GAP+\bar{p}^{(*)}$, where X is a specific central state and GAP is a region of rapidity where no particles are detected ($1.3 < |\eta| < 5.9$). We do not detect outgoing (anti)protons, thus events where they dissociate into hadrons, $p \to p^*$, with $|\eta| > 5.9$ are also included. The highlights of our analysis have been recently published in [3].

The exclusive central hadronic systems resulting primarily from double pomeron exchange have very restrictive quantum numbers: $I^G J^{PC} = 0^+(\text{even})^{++}$. This "quantum number filter" is a powerful tool for meson spectroscopy in the isoscalar sector, especially for glue-rich states. In addition it provides information on the nature of the pomeron.

[a] e-mail: m.zurek@fz-juelich.de

Operated by Fermi Research Alliance, LLC under Contract No. De-AC02-07CH11359 with the United States Department of Energy

2 Experimental Setup

The CDF II detector setup, located at the Fermi National Accelerator Laboratory, is a general purpose detector designed to study $p\bar{p}$ collisions at the Tevatron ring. The setup is described with details in [4]. Here, a short overview of the detectors used in the analysis is given. The $p\bar{p}$ interaction point is surrounded by silicon microstip detectors and a drift chamber in a 1.4 Tesla magnetic field provided by a solenoid. These detectors compose together a tracking system with almost 100% track reconstruction efficiency for particles with $p_T > 0.4$ GeV/c and $|\eta| < 1.3$. The drift chamber is surrounded by a time-of-flight (TOF) counters barrel, consisting of plastic scintillator bars, read out at both ends by photomultipliers. The TOF detectors cover $|\eta| < 0.9$. Electromagnetic (EM) and hadronic (HAD) calorimeters are installed just after the solenoid. Both the central part of the calorimeters ($|\eta| < 1.32$) and forward plugs ($1.32 < |\eta| < 3.64$) have pointing tower geometry. To monitor the luminosity and veto events with particles in the region $3.7 < |\eta| < 4.7$, gas Cherenkov counters (CLC) were used. Beam shower counters (BSC) covering $5.4 < |\eta| < 5.9$ consist of 1.7 radiation lengths of lead and scintillation counters. The region between $4.7 < |\eta| < 5.4$ stays uninstrumented, giving a contribution to the nonexclusive background.

The data were taken with two different center-of-mass energies, with $\sqrt{s} = 1.96$ TeV and during a special low pile-up run with $\sqrt{s} = 0.9$ TeV. The beam proton rapidities at two center-of-mass energy values are $y_{\text{beam}} = 6.87$ and 7.64 respectively. Since we do not register outgoing (anti)protons, data include diffraction dissociation processes. At $\sqrt{s} = 1.96$ TeV higher dissociation masses are allowed than at 0.9 TeV.

3 Event Selection

The dedicated trigger requires two or more central ($|\eta| < 1.3$) calorimeter towers (EM + HAD) with $E_T > 0.5$ GeV and a veto on BSC, CLC and forward plug calorimeter. The trigger was activated when the mean pile-up was low.

In our analysis we use events with no pile-up and exactly two charged particles in a central region with $|\eta| < 1.3$ and $p_T > 0.4$ GeV/c, with no other particles in the detector, to $|\eta| < 5.9$. We assume that there is no particle in the detector when its readout signal is consistent with noise. To define the noise level unbiased bunch-crossing trigger data (zero-bias) are used. The zero-bias events are divided into two subgroups (a) in which no tracks or CLC hits are detected, (b) all other events, which are dominated by one or more interactions. Comparing the readout for the noise and signal-dominated samples, the noise level is determined for each subdetector. We apply a cut both on the sum of all signals $\sum(EM + HAD)$ and on the highest $E_T(EM)$ tower in each event, for each of the subdetectors. In the central region, tracks are extrapolated to the calorimeters. We require all calorimeter elements to have the pulse height consistent with the noise, apart from the cones $\sqrt{(\Delta\eta)^2 + (\ Delta\phi)^2} < 0.3$ around the track extrapolation point.

An opening-angle cut and a requirement of zero muons eliminate the small background from cosmic ray tracks. Charged-particle track quality cuts are applied. The tracks are required to have at least 25 hits in both stereo and axial layers of the drift chamber, and a fit with $\chi^2/\text{DoF} < 2.5$. They both have to pass within 0.5 mm of the beam line in the transverse plane and to be within 1 cm of each other in z at that point. The measured particles are required to have opposite charge. We assume both particle to be pions and we put the requirement of $|y(\pi\pi)| < 1.0$.

4 Effective luminosity

In our analysis, we use only events with no other visible interaction to spoil the exclusivity. To obtain the effective integrated luminosity L_{eff}, the probability of having no pile-up, called the exclusive

efficiency $\varepsilon_{\rm eff}$, has to be calculated. Using the zero-bias data, we calculate the probability that the full detector is empty, as a function of the individual bunch integrated luminosity $L_{\rm bunch}$. The distribution is exponential $\varepsilon_{\rm eff} = e^{-\sigma_{\rm vis} L_{\rm bunch}}$ with the intercept consistent with 1.0. The slope, $\sigma_{\rm vis}$, is the total observed ($|\eta| < 5.9$) cross-section. We find $\sigma_{\rm vis} = 55.9 \pm 0.4$ mb at 1.96 TeV. It is consistent with an expectation from global fits [5] of total inelastic cross-section $\sigma_{\rm inel} = 61.0 \pm 1.8$ mb, corrected for the estimated part visible in the region $|\eta| < 5.9$, $\sigma_{\rm vis}/\sigma_{\rm inel} = 0.85 \pm 0.05$ [6], which gives $\sigma_{\rm vis}$(expected) $= 51.8 \pm 3.4$ mb. We find $L_{\rm eff} = 1.16$ pb^{-1}, for $\sqrt{s} = 1.96$ TeV, with about 6.7% uncertainty.

For $\sqrt{s} = 0.9$ TeV the CLC counters were not calibrated to the luminosity. Therefore, we use $\sigma_{\rm vis}$ to calibrate the overall luminosity. The expected observed cross-section $\sigma_{\rm vis}$(expected) is obtained from the total inelastic cross-section [5], $\sigma_{\rm inel} = 52.7 \pm 1.6$ mb, multiplied by an estimate [6] of $\sigma_{\rm vis}/\sigma_{\rm inel} = (0.90 \pm 0.05)$. Comparing the value of $\sigma_{\rm vis}$ from the fit to the zero-bias data to expected one, the correction factor for the $\sqrt{s} = 0.9$ TeV luminosity is determined. The final value of the effective integrated luminosity equals $L_{\rm eff} = 0.059$ pb^{-1} with about 10% uncertainty.

5 Acceptance calculation

All calculated differential cross-sections are required to be in a certain kinematic region, namely $|\eta(\pi)| < 1.3$, $p_T(\pi) > 0.4$ GeV/c, and $|y(\pi\pi)| < 1.0$. The transverse momentum and pseudorapidity requirements allow to accept only well-reconstructed tracks, and the y cut defines the rapidity gap. The acceptance combined with cut efficiency is a function of single track $p_T(\pi)$, $\eta(\pi)$; the invariant mass of two pions $M(\pi\pi)$; and p_T of the central $\pi\pi$ state.

The trigger efficiency is based on a data-driven procedure, using well-measured isolated tracks from minimum-bias data. Probabilities of triggering 0, 1, 2 or more towers with $\sum E_T \geq 0.5$ GeV in the region around the track extrapolation are calculated. The total trigger efficiency as a function of p_T and η of the track is composed of those three contributions.

The acceptance and cut efficiency as a function of $p_T(\pi)$ and $\eta(\pi)$ is calculated using simulated single pions. After detector simulation using a GEANT-3 Monte Carlo program [7], the track reconstruction probability is determined. As a next step, the simulated track is checked to pass all the quality requirements. The single track acceptance is fitted with a smooth empirical function.

Since the acceptance is dependent not only on single track features, but also on correlations between two tracks, the additional acceptance component as a function of $M(\pi\pi)$ and $p_T(\pi\pi)$ is determined. For that reason, a parent state is generated in mass bins from $2M(\pi)$ to 5000 MeV/c^2 and p_T bins from 0 to 2.5 GeV/c. The central state decays isotropically (S-wave, J=0). A bilinear interpolation to compute the acceptance at every point is used, to avoid fake structures from statistical fluctuations in the Monte Carlo.

6 Background estimation

A background from hadron pairs that are not $\pi^+\pi^-$ is determined using the information from the TOF counters. The time-of-flight information is available when both particles are in a region $|\eta| < 0.9$. Consequently, only 67% of all pairs have both particles identified. For this sample of events, (89±1)% are $\pi^+\pi^-$. When both tracks are in a region $|\eta| < 0.7$, then about 90% of the hadron pairs are identified. For two different regions of η, $|\eta| < 0.7$ and $|\eta| < 0.9$, no significant change in the composition of the identified particle types is observed. All the spectra include non-$\pi^+\pi^-$ background. We assign pion masses for all measured hadron pairs.

The events with two same-charged hadrons are 6.1% and 7.1% at 0.9 TeV and 1.96 TeV respectively, and are rejected. They are an indication of nonexclusive background with at least two untagged

charged particles, either below the p_T-threshold, or because of inefficiency with no energy above the noise level in the calorimeters or no reconstructed track. We expect there to be a similar number of same charge events with missed tracks.

7 Cross-sections

The differential cross-section as a function of $M(\pi\pi)$ and $p_T(\pi\pi)$ is presented in Fig. 1. To avoid the region with zero acceptance we present the total cross-section as a function of invariant mass of two pions in the range 1000 MeV/c^2 < $M(\pi\pi)$ < 5000MeV/c^2 integrated over all $p_T(\pi\pi)$ (Figs. 2, 3), and in the range 300 MeV/c^2 < $M(\pi\pi)$ < 5000 GeV/c^2 for $p_T(\pi\pi)$ > 1 GeV/c (Fig. 4).

In Figs. 2, 3 a peak centered at 1270 MeV/c^2 with a full-width at half-maximum ~200 MeV/c^2 is visible. It is consistent with the $f_2(1270)$ state. The shoulder on the high-mass side of the $f_2(1270)$ can be evidence of the $f_0(1370)$ meson. A change of slope in the cross-section distribution at 1500 MeV/c^2 is seen. In this region, at lower $\sqrt{s}$, a dip was observed. It is possibly caused by interference between resonances [10, 11]. At higher masses up to 2400 MeV/c^2, there are structures in the mass distribution, suggesting the production of other resonances. As shown in Fig. 3, the data fall monotonically with $M(\pi\pi)$ from 2000 to 5000 MeV/c^2. The small peak at 3100 MeV/c^2 is consistent with $J/\psi \to e^+e^-$ photoproduction [12]. In Fig. 3 the predictions from the DIME Monte Carlo [13] of the differential cross-section for the mass region $M(\pi\pi)$ > 2600 MeV/c^2 are presented. The large uncertainties of the predictions have their origin in the unknown $\pi\pi\,\mathbb{P}$ form factor. The MC with an exponential form factor agrees with the data at 3000 MeV/c^2. However, a steeper $M(\pi\pi)$ dependence is predicted.

The ratio of the differential cross-section for two different $\sqrt{s}$, $R(0.9 : 1.96)$, presented in Fig. 2, rises from about 1.2 at 1000 MeV/c^2 to about 2.0 at 4000 MeV/c^2 with no significant structures. The ratio expected by Regge phenomenology when both protons are intact should be equal to approximately 1.3 [2, 8, 9]. For 1000 < $M(\pi\pi)$ < 2000 MeV/c^2 it is $R(0.9 : 1.96) = 1.284 \pm 0.039$. Our data include dissociation, with higher masses allowed at $\sqrt{s}$ = 1.96 TeV. For 2000 < $M(\pi\pi)$ < 3000 MeV $R(0.9 : 1.96) = 1.560 \pm 0.056$.

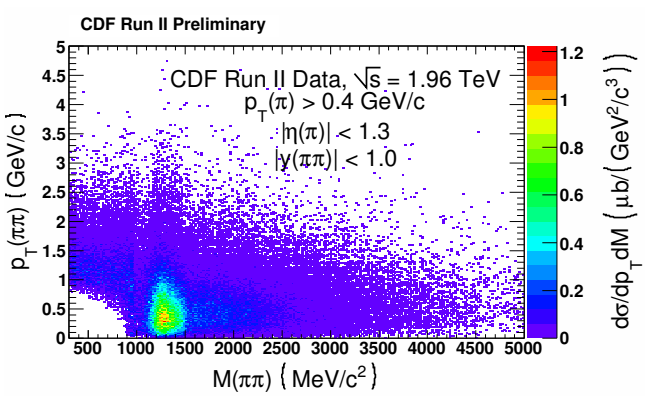

Figure 1. Differential cross-section $d\sigma/dM(\pi\pi)dp_T(\pi\pi)$ for two charged particles, assumed to be $\pi^+\pi^-$, with p_T > 0.4 GeV/c, $|\eta|$ < 1.3 and $|y(\pi\pi)|$ < 1.0 between two rapidity gaps 1.3 < $|\eta|$ < 5.9. (Colour online)

The differential cross-section for $p_T(\pi\pi)$ > 1000 MeV/c^2 is presented in Fig. 4. The distribution is flat up to a sharp drop at $M(\pi\pi)$ = 1000 MeV/c^2, where the $f_0(980)$ and the K^+K^- threshold occur. The drop was seen in previous experiments [2].

The distribution of mean $p_T(\pi\pi)$ as a function of $M(\pi\pi)$, shown in Fig. 5, shows a significant local rise at $M(\pi\pi) \approx 1500$ MeV/c^2, coinciding with the change in slope of the differential cross-section (Figs. 2 and 3), followed by a trend to larger values at higher mass.

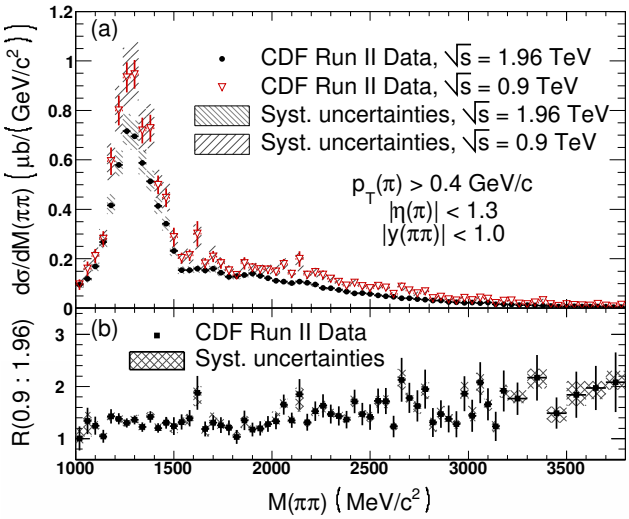

Figure 2. (a) Differential cross-section $d\sigma/dM(\pi\pi)$ for two charged particles, assumed to be $\pi^+\pi^-$, with $p_T > 0.4$ GeV/c, $|\eta| < 1.3$ and $|y(\pi\pi)| < 1.0$ between two rapidity gaps $1.3 < |\eta| < 5.9$. Red open circles for $\sqrt{s}$ = 0.9 TeV and black points for $\sqrt{s}$ = 1.96 TeV. (b) Ratio of cross-sections at $\sqrt{s}$ = 0.9 and 1.96 TeV. Source [3].

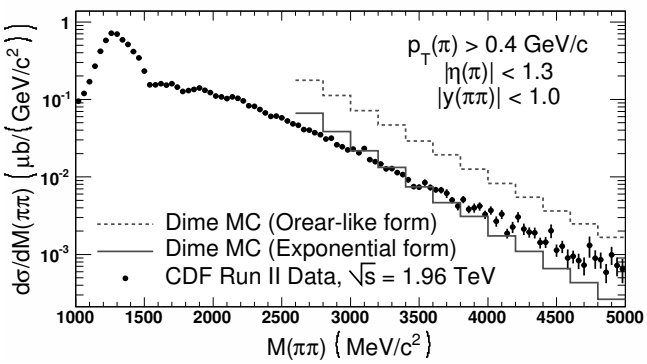

Figure 3. Differential cross-section $d\sigma/dM(\pi\pi)$ at $\sqrt{s}$ = 1.96 TeV for two charged particles, assumed to be $\pi^+\pi^-$, with $p_T > 0.4$ GeV/c, $|\eta| < 1.3$ and $|y(\pi\pi)| < 1.0$ between two rapidity gaps $1.3 < |\eta| < 5.9$. Only statistical errors are shown; systematic uncertainties contribute approximately 10% at all masses. The lines show predictions of Ref. [13] with two different pion form factors. Source [3].

Summing up, the exclusive $\pi^+\pi^-$ differential cross-section has been measured, with $|y(\pi\pi)| < 1.0$ and rapidity gaps out to $|\eta(\pi\pi)| < 5.9$, at two $p\bar{p}$ centre of mass energies, $\sqrt{s}$ = 0.9 and 1.96 TeV. The differential cross-section shows a sharp drop at 1000 MeV/c^2, a strong $f_2(1270)$ resonance enhancement, and other features at higher mass, the origin of which is uncertain.

8 Acknowledgments

I would like to thank my CDF colleagues, especially Mike Albrow (Fermilab). I thank the ISMD2015 Organizing Committee and Bonn-Cologne Graduate School for Physics and Astronomy for the student allowance.

References

[1] See, e.g., J.R. Forshaw and D.A. Ross, *Quantum Chromodynamics and the Pomeron*, Cambridge Lecture Notes in Physics (Cambridge University Press, Cambridge, England, 1997); S. Donnachie, G. Dosch, P. Landshoff, and O. Nachtmann, *Pomeron Physics and QCD* (Cambridge University Press, Cambridge, England, 2002).

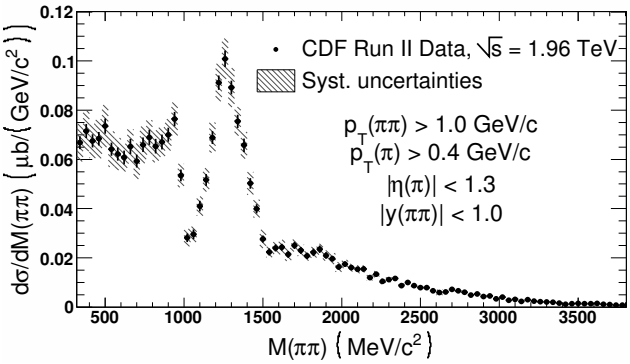

Figure 4. As Fig. 2 at $\sqrt{s}$ = 1.96 TeV, but with $p_T(\pi\pi) > 1.0$ GeV/c for which the acceptance extends to low $M(\pi\pi)$. Source [3].

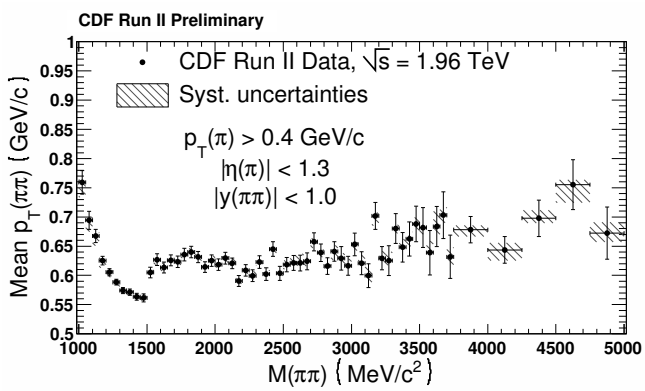

Figure 5. Mean value of the p_T distribution of the central state decaying to two pions, corrected for acceptance, as a function of $M(\pi\pi)$ at $\sqrt{s}$ = 1.96 TeV.

[2] See, e.g., M.G. Albrow, T.D. Coughlin, and J.R. Forshaw, Prog. Part. Nucl. Phys. **65**, 149 (2010); M.G.Albrow, Int. J. Mod. Phys. A **29**, 1402006 (2014) and references therein.

[3] T. Aaltonen *et al.* (CDF Collaboration) Phys. Rev. D **91**, 091101 (2015).

[4] D. Acosta *et al.* (CDF Collaboration), Phys. Rev. D **50**, 2966 (1994) and references therein; F. Abe *et al.* (CDF Collaboration), Nucl. Instrum. Methods Phys. Res., Sect. A **271**, 387 (1988).

[5] G. Antchev *et al.* (TOTEM Collaboration), Europhys. Lett. **101**, 21002 and 21004 (2013); Phys. Rev. Lett. **111**, 012001 (2013).

[6] R. Ciesielski and K. Goulianos, Proc. Sci., ICHEP **2012**, 301 (2013).

[7] R. Brun, R. Hagelberg, M. Hansroul, and J.C. Lassalle, GEANT version 3.15, Report No. CERN-DD-78-2-REV.

[8] Y.I. Azimov, V.A. Khoze, E.M. Levin and M.G. Ryskin, Sov. J. Nucl. Phys. **21**, 215 (1975).

[9] B.R. Desai, B.C. Shen, and M. Jacob, Nucl. Phys. **B142**, 258 (1978).

[10] See, e.g., T. Åkesson *et al.* (AFS Collaboration), Nucl. Phys. **B264**, 154 (1986).

[11] A. Breakstone *et al.*, Zeit. Phys. C **31**, 185 (1986).

[12] T. Aaltonen *et al.* (CDF Collaboration) Phys. Rev. Lett. **102**, 242001 (2009).

[13] L.A. Harland-Lang, V.A. Khoze, and M.G. Ryskin (DIME MC), Eur. Phys. J. C **74**, 2848 (2014).